L-4F Differentially Alters Plasma Levels of Oxidized Fatty Acids Resulting in more Anti-Inflammatory HDL in Mice

Satoshi Imaizumi[1], Victor Grijalva[1], Mohamad Navab[1], Brian J. Van Lenten[1], Alan C. Wagner[1], G.M. Anantharamaiah[2], Alan M. Fogelman[1], and Srinivasa T. Reddy[1,*]

[1]*Departments of Medicine, David Geffen School of Medicine at UCLA, Los Angeles, CA 90095-1679, USA and the Atherosclerosis Research Unit, Department of Medicine,* [2]*University of Alabama at Birmingham, Birmingham, AL 35294, USA*

Abstract: To determine *in vivo* if L-4F differentially alters plasma levels of oxidized fatty acids resulting in more anti-inflammatory HDL. Injecting L-4F into apoE null mice resulted in a significant reduction in plasma levels of 15-HETE, 5-HETE, 13-HODE and 9-HODE. In contrast, plasma levels of 20-HETE were not reduced and plasma levels of 14,15-EET, which are derived from the cytochrome P450 pathway, were elevated after injection of L-4F. Injection of 13(*S*)-HPODE into wild-type C57BL/6J mice caused an increase in plasma levels of 13-HODE and 9-HODE and was accompanied by a significant loss in the anti-inflammatory properties of HDL. The response of atherosclerosis resistant C3H/HeJ mice to injection of 13(*S*)-HPODE was similar but much more blunted. Injection of L-4F at a site different from that at which the 13(*S*)-HPODE was injected resulted in significantly lower plasma levels of 13-HODE and 9-HODE and significantly less loss of HDL anti-inflammatory properties in both strains. i) L-4F differentially alters plasma levels of oxidized fatty acids *in vivo*. ii) The resistance of the C3H/HeJ strain to atherosclerosis may in part be mediated by a reduced reaction of this strain to these potent lipid oxidants. L-4F differentially alters plasma levels of oxidized fatty acids in mice and the resistance of C3H/HeJ mice to atherosclerosis may be mediated by a reduced reaction of this strain to these potent lipid oxidants.

Keywords: HETE, HODE, HPODE, EET, apoA-I mimetic peptides, L-4F, arachidonic acid metabolism.

INTRODUCTION

Atherosclerosis is the result of complex interactions between oxidized lipoproteins, monocytes/macrophages, injured endothelium, and smooth muscle cells. Biological oxidation products of arachidonic acid, including prostaglandins (PGs), thromboxanes (TXs), hydroxyeicosatetraenoic acids (HETEs) and hydroxyoctadecadienoic acids (HODEs) play an important role in the pathogenesis of atherosclerosis. The biosynthesis of most eicosanoids (HETEs, PGs, TXs) from arachidonic acid occurs via lipoxygenase (LOX), cyclooxygenase (COX) and cytochrome P450 pathway (CYP) enzymes. LOX are classified as 5-, 8-, 12-, and 15-LOX according to the positional specificity to insert molecular oxygen at corresponding positions of arachidonic acid. The 5- and 8-LOX pathway leads to the formation of S hydroperoxyeicosatetraenoic acid (HPETE) isomers from arachidonic acid, namely 5(*S*)-hydroperoxyeicosatetraenoic acid (5(*S*)-HPETE) and 8(*S*)-HPETE respectively, and the 12- and 15-LOX pathway leads to the formation of 12(*S*)-HPETE or 15(*S*)-HPETE. With linoleic acid, 12- and 15-LOX form S hydroperoxyoctadecadienoic acids [13(*S*)- and 9(*S*)-HPODE]. These HPETEs and HPODEs are subsequently reduced to their hydroxyl derivatives HETEs and HODEs. The 12- and 15-LOX pathway has been shown to oxidize LDL *in vitro* [1, 2].

*Address correspondence to this author at the 3736 MRL, Department of Medicine/Cardiology, Department of Molecular and Medical Pharmacology, University of California Los Angeles, 650 Charles E. Young Drive South, Los Angeles, CA 90095, USA; Tel: (310) 825-9930; Fax: (310) 206-0589; E-mail: sreddy@mednet.ucla.edu

LDL oxidation is a complex process that can also be influenced by a multitude of oxidation pathways including peroxidase, peroxynitrite, xanthine oxidase, NADPH oxidase and superoxide [3]. One of the major pathways of LDL oxidation occurs *via* the LOX pathway by seeding molecules that include HPODE and HPETE [4, 5]. The oxidation of polyunsaturated fatty acids (PUFA) by LOX specifically produces the S enantiomer (e.g. 13(S)-HPODE), whereas non-enzymatic PUFA oxidation yields equal amounts of R and S stereoisomers (e.g. 13(S)-HPODE and 13(R)-HPODE) [6, 7]. This stereospecificity was used as marker of LOX activity [6, 8]. Studies in rabbits fed a cholesterol-rich diet and in humans reported both 13(S)-H(P)ODE and 13(R)-H(P)ODE in atherosclerotic lesions with 13(S)-H(P)ODE as the predominant type, suggesting that both LOX enzyme mediated lipid oxidation and non-enzymatic lipid oxidation mechanisms exist *in vivo* [6, 8]. 12/15-LOX/apoE double knock out mice develop reduced atherosclerotic lesions when compared to apoE deficient mice [9]. 12/15-LOX/LDL-R double knockout mice on a high-fat diet also had a considerable reduction in atherosclerotic lesions when compared to LDL-R knockout mice [10]. In human aortic endothelial cells (HAECs), 12(*S*)-HETE and 15(*S*)-HETE induced monocyte adhesion and increased HAEC surface expression of connecting segment-1 fibronectin, which plays a role in monocyte adhesion during inflammation [11].

The cytochrome P450 pathway also leads to the production of HETEs from arachidonic acid, including 20-HETE, and non-ezymatic, free radical oxidation of arachidonic acid

1872-3128/10 $55.00+.00

can yield a variety of oxidized lipids including 9-HETE. In human unstable carotid atherosclerotic plaques compared with stable plaques, 9-HETE was significantly increased [12], and the systemic level of 9-HETE was associated with angiographic evidence of coronary artery disease [13]. 20-HETE is a potent vasoconstrictor that can modulate renal function and peripheral vascular tone [14]. The cytochrome P450 pathway also converts arachidonic acid to epoxyeicosatrienoic acids (EETs) which produce vascular relaxation and have anti-inflammatory effects on blood vessels [15]. Thus, oxidized fatty acids derived from arachidonic acid or linoleic acid are associated with diverse effects in the vasculature and be either pro-inflammatory or anti-inflammatory.

The apolipoprotein A-I mimetic peptide 4F (L-4F and D-4F), forms a class A amphipathic helix similar to those found in apoA-I, and has been reported to have anti-inflammatory and anti-atherogenic effects [16]. *In vitro* and *in vivo* 4F has been shown to reduce plasma lipid hydroperoxide concentrations, which are predominantly derivatives of linoleic and arachidonic acid [16]. We previously reported that *in vitro* apoA-I and the 4F peptides bound non-oxidized fatty acids such as arachidonic acid and linoleic acid similarly, but the 4F peptides bound oxidized fatty acids derived from arachidonic acid or linoleic acid with an astoundingly higher affinity than apoA-I [17]. For instance, the binding affinity of 15-HPETE, 15-HETE, 13-HPODE and 13-HODE were 4-5 orders of magnitude higher for binding to 4F compared to apoA-I as measured by surface plasmon resonance [17].

The *in vivo* effects of 4F on oxidized fatty acids have not been elucidated to date. In this paper, we sought to determine if L-4F would differentially alter plasma levels of oxidized fatty acids and would result in more anti-inflammatory HDL. In the course of these experiments we also determined the susceptibility of atherosclerosis prone C57BL/6J mice compared to atherosclerosis resistant C3H/HeJ mice to *in vivo* challenge with the potent fatty acid hydroperoxide 13(*S*)-HPODE. These studies demonstrate that L-4F differentially alters plasma levels of oxidized fatty acids *in vivo* and also suggest that the resistance of C3H/HeJ mice to atherosclerosis may be due to their blunted response to these potent lipid oxidants.

MATERIALS AND METHODS

Chemicals and Materials

(±)13-hydroxy-9Z,11E-octadecadienoic acid (13-HODE), (±)9-hydroxy-10E,12E-octadecadienoic acid (9-HODE), (±) 15-hydroxy-5Z,8Z,11Z,13E-eicosatetraenoic acid (15-HETE), (±)5-hydroxy-6E,8E,11Z,14Z-eicosatetraenoic acid (5-HETE), 20-hydroxy-5Z,8Z,11Z,14Z-eicosatetraenoic acid (20-HETE), 13(S)-hydroperoxy-9Z,11E-octadecadienoic acid (13(S)-HPODE), 15(S)-hydroxy-5Z,8Z,11Z,13E-eicosatetraenoic-5,6,8,9,11,12,14,15-d_8 acid (15(S)-HETE-d8), 13 (S)-hydroxy-9Z,11E-octadecadienoic-9,10,12,13-d_4 acid (13 (S)-HODE-d4), (±)14,15-epoxy-5Z,8Z,11Z-eicosatrienoic acid ((±)14,15-EET) were purchased from Cayman Chemicals (Ann Arbor, MI, USA). HPLC grade methanol was obtained from Sigma-Aldrich (St. Louis, MO, USA). HPLC grade acetonitrile was obtained from Fisher Scientific (Pittsburgh, PA, USA). Oasis HLB (1cc/10mg, 30µm) was purchased from Waters Corporation (Milford, MA, USA). L-4F and D-4F were synthesized as previously described [18, 19]. Dichlorofluorescein diacetate (H_2DCFDA) was from Invitrogen (Carlsbad, CA, USA). 8-bromoadenosine 3',5'-cyclic monophosphate sodium salt (8-bromo-cAMP) was purchased from Sigma. All other reagents were HPLC grade.

Mice

Female 8 to 10 months old C57BL/6J mice, apoE null mice on a C57BL/6J background, and C3H/HeJ mice (Jackson Laboratories, Bar Harbor, ME) were maintained on a chow diet (Ralston Purina, St. Louis MO). Plasma samples were isolated from overnight fasted mice and immediately frozen at -20°C until they were used. The University of California, Los Angeles Animal Research Committee approved all studies.

Sample Preparation

A 100µL volume of plasma sample or 50µL volume of urine sample was transferred to a 2mL polypropylene tube, and spiked with 100µL of internal standards mixture (15(S)-HETE-d8, 13(S)-HODE-d4, 10ng/ml each) in methanol. Subsequently, the pH of the samples was adjusted to ~ pH 3.0 using acidified (HCl) water. The samples were left for 15min on ice for complete acidification and equilibration. For analysis of plasma total (free + esterified) HETEs/ HODEs in supplemental Fig. (**7**) the samples were hydrolyzed with 1mol/L potassium hydroxide in water at 37°C for 30 minutes before the acidification. The resulting sample was loaded onto a preconditioned 1cc Oasis HLB solid-phase extraction (SPE) cartridge on a vacuum manifold (Waters). The SPE cartridge was equilibrated with 1ml methanol followed by 1ml water before the sample load. The sample was slowly loaded on the cartridge, and the cartridge was washed with 1ml 5% methanol in water. HETEs/HODEs, 14,15-EET and arachidonic acid were subsequently eluted with 1 ml methanol. The eluate was then evaporated to dryness under a stream of argon. 100µl of methanol was added to the dried extract, vortexed for 30s, and the reconstituted extract was centrifuged at 13,200 rpm for 20min at 4°C to remove any precipitate that could clog the LC/MS/MS instrument. The resulting supernatants were transferred to autosampler vials and processed for LC/MS/MS analysis.

For quantification of HETEs/HODEs in Fig. (**3**) 300µl of chloroform/methanol (2:1, v/v) containing 0.01% BHT was added to 100µl plasma [20, 21]. After the solution was thoroughly mixed and centrifuged, the lower chloroform phase was collected. Additional chloroform was added to the upper phase to remove residual lipids. The solution was mixed and centrifuged, and the lower phase was transferred to the previously isolated chloroform phase.

LC/MS/MS Analysis

LC/MS/MS was performed using a mass spectrometer (4000 QTRAP; Applied Biosystems, Foster City, CA) equipped with electrospray ionization (ESI) source. The HPLC system utilized an Agilent 1200 series LC pump equipped with a thermostatted autosampler (Agilent Technologies, Santa Clara, CA). Chromatography was performed

using a Luna C-18(2) column (3µm particle, 150 × 3.0mm; Phenomenex, Torrance, CA) with a security guard cartridge (C-18; Phenomenex) at 40°C. Mobile phase A consisted of 0.1% formic acid in water, and mobile phase B consisted of 0.1% formic acid in acetonitrile. The auotosampler was set at 4°C. The injection volume was 10µl except for (±)14,15-EET when 50µl was injected; the flow rate was controlled at 0.4mL/min. The gradient program was as follows: 0-2min, 50% B; 2-3min, linear gradient from 50% to 60% B; 3-15min, linear gradient from 60-65% B; 15-17min, 65% B; 17-19min, linear gradient from 65-100% B; 19-21min 100% B; 21-23min, linear gradient from 100% to 50% B; 23-27min, 50% B. The data acquisitions and instrument control were accomplished using Analyst 1.4.2 software (Applied Biosystems). Detection was accomplished by using the multiple reaction monitoring (MRM) mode with negative ion detection; the parameter settings used were: ion spray voltage=-4500 V; curtain gas=25 (nitrogen); ion source gas 1=45; ion source gas 2 =55; ion source gas 2 temperature=450°C. Collision energy, declustering potential and collision cell exit potential were optimized for each compound to obtain optimum sensitivity. The transitions monitored were mass-to-charge ratio (m/z): m/z 295.1→194.8 for 13-HODE; 295.0→171.0 for 9-HODE; 319.1→219.0 for 15-HETE; 319.1→115.0 for 5-HETE; 319.1→289.2 for 20-HETE; 319.0→219.0 for 14,15-EET; 327.1→226.1 for 15(*S*)-HETE-d_8; 299.0→197.9 for 13(*S*)-HODE-d_4; 310.9 →166.5 for 13(S)-HPODE, 303.1→259.2 for arachidonic acid.

Measurement of 15-HETE and 20-HETE by ELISA

Plasma 15-HETE was measured by using the 15(*S*)-HETE EIA kit (Cayman). Plasma 20-HETE was measured by using the 20-HETE EIA kit (Detroit R&D). The data on the specificity of each ELISA kit were obtained from each company.

Assays to Determine the Inflammatory Properties of HDL

HDL inflammatory properties were determined as previously described by using H_2DCFDA [22] and the ability of HDL to inhibit LDL-induced monocyte chemotactic activity in cultures of human aortic endothelial cells using a bioassay [23].

Lipid Binding Studies

Binding studies were performed by surface plasmon resonance (SPR) as previously described [17].

Electrophoresis

SDS-PAGE and native-PAGE were performed as described previously [24].

HDL Mediated Cellular Cholesterol Efflux

Experiments were performed as described previously [25]

Blood and Urine Chemistry

Blood samples were examined for total protein and albumin and urine samples were examined for creatinine by an autoanalyzer (Alfa Wassermann VetAce; Alfa Wassermann Diagnostic Technologies, West Caldwell, NJ).

Statistical Analysis

All statistical analysis was calculated using an unpaired Student's t-test or one-way ANOVA. Significance was defined as a value of $p < 0.05$. If unstated, all values are expressed as Mean ± SD.

RESULTS

Comparison of HETEs/HODEs between ApoE$^{-/-}$ Mice and C57BL/6J Mice

The levels of HETEs/HODEs in plasma from atherosclerosis-prone apolipoprotein E knock out mice on a C57BL/6J background (ApoE$^{-/-}$ mice) compared to wild-type C57BL/6J mice were determined. As shown in Fig. (**1**) the plasma levels of HETEs/HODEs from the ApoE$^{-/-}$ mice were significantly higher than in the wild-type C57BL/6J mice confirming previously published data [26].

Lipid Binding Studies

We previously reported that a variety of oxidized fatty acids derived from either arachidonic or linoleic acid bound with much higher affinity to the 4F peptide compared to apoA-I [17]. In measuring binding affinity K*D* = Kd/Ka where Kd is the dissociation rate constant and Ka is the association rate constant. The larger the K*D* is, the weaker the binding. We previously reported that the K*D* for the binding of 15-HETE to L-4F and apoA-I was 21 ± 7 and 1,289,400 ± 139,245 nM, respectively; the K*D* for the binding of 13-HODE to L-4F and apoA-I was 32 ± 4 and 1,803,400 ± 279,731 nM, respectively; the K*D* for the binding of 9-HODE to L-4F and apoA-I was 26 ± 11 and 1,312,200 ± 534,323 nM, respectively [17]. For this manuscript, new data were obtained from 5 separate experiments revealing that the K*D* for the binding of 20-HETE to L-4F and apoA-I was 164,000 ± 8,210 and 172,000 ± 8,610 nM, respectively. Thus, in contrast to the case for 15-HETE, 13-HODE and 9-HODE, 20-HETE binds equally well to L-4F and apoA-I.

Plasma Levels of Oxidized Fatty Acids after L-4F Administration

After subcutaneous administration of 1mg/kg L-4F to apoE null mice, the plasma concentration of 15-HETE determined by ELISA decreased in a time dependent manner with significant differences detected 4, 6, and 12 hours after injection Fig. (**2a**). In another experiment, L-4F at 1 mg/kg or vehicle alone (ABCT) was administered to apoE-null mice and the plasma concentrations of 15-HETE and 20-HETE were determined by ELISA 6 hours later. As shown in Fig. (**2b**) administration of L-4F but not vehicle significantly reduced plasma 15-HETE levels. However, in same group of mice, plasma 20-HETE levels were not changed by L-4F administration Fig. (**2c**). There was no cross-reactivity of 20-HETE in the 15-HETE ELISA and 15-HETE in the 20-HETE ELISA (Supplemental Table **1**). We also checked the effect of L-4F on 15-HETE ELISA in the presence of mouse plasma and found no effect of L-4F on the 15-HETE ELISA (Supplemental Fig. (**1**)).

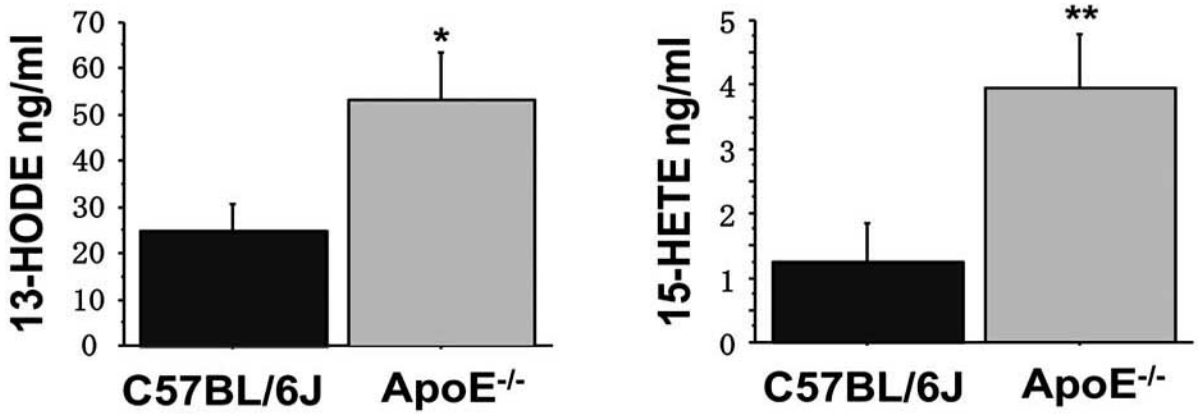

Fig. (1). Plasma 13-HODE and 15-HETE levels in wild-type and apoE null mice. The levels of plasma 13-HODE and 15-HETE in apolipoprotein E null mice on a C57BL/6J background (ApoE$^{-/-}$ mice) and wild-type C57BL/6J mice (both on a chow diet) were analyzed by LC/MS/MS as described in Materials and Methods. (n=6 for each group).

* P=0.0001 vs. C57BL/6J mice. * *P<0.0001 vs. C57BL/6J mice.

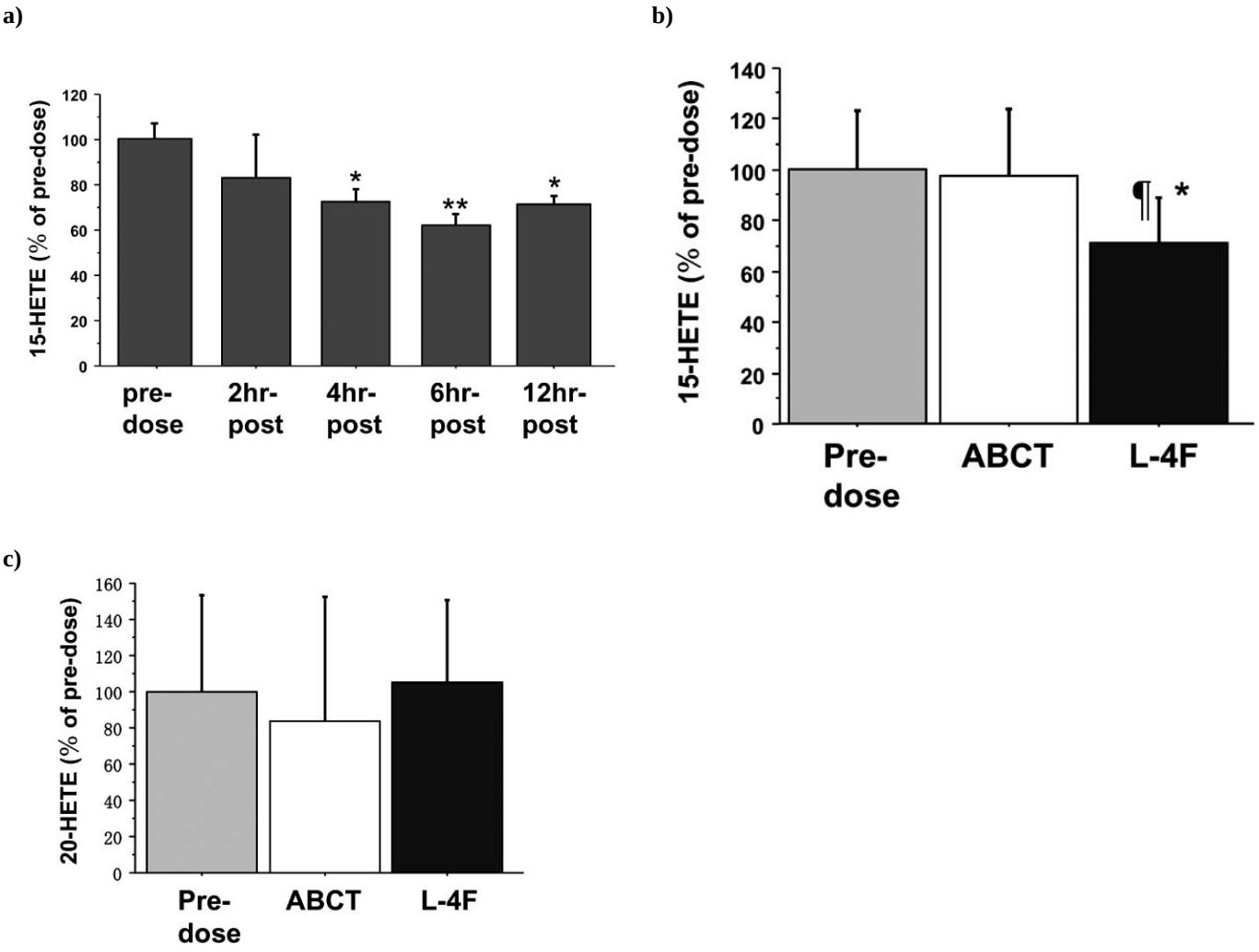

Fig. (2). L-4F treatment differentially reduces plasma HETEs levels as measured by ELISA. **Panel a)** ApoE null mice were injected subcutaneously with L-4F at 1 mg/kg and were bled at the time points shown in the figure and plasma 15(*S*)-HETE levels were determined by ELISA. * P<0.05 vs. pre-dose. ** P<0.01 vs. pre-dose. n=3, each time point. **Panels b** and **c)** ApoE null mice were administered subcutaneously vehicle (ABCT) (50 mM ammonium bicarbonate, pH 7.0 containing 0.1 mg/mL Tween-20) or vehicle containing L-4F at a dose of 1 mg/kg. After six hours, plasma **b)** 15-HETE (n=12 each group) and **c)** 20-HETE levels (n=6 each group) were determined by ELISA and compared to pre-dose levels. ¶p=0.0038 vs. pre-dose. *p=0.0081 vs. ABCT alone.

In additional experiments as shown in Fig. (**3**) plasma levels of 13-HODE and 9-HODE Fig. (**3a**) and 15-HETE and 5-HETE Fig. (**3b**) significantly declined 6 hours after injection of L-4F as determined by LC/MS/MS but not after injection of vehicle alone. In these repeat experiments using LC/MS/MS, as was the case in the experiments in Fig. (**2**) where plasma levels of 20-HETE were determined by ELISA, the levels of 20-HETE did not decline Fig. (**3b**).

As shown in Fig. (**3c**) subcutaneous administration of 1mg/kg L-4F to apoE-null mice significantly *increased* the plasma levels of 14,15-EET. Although the mass-to-charge ratio (m/z) monitored for 15-HETE (319.1→219.0) and 14,15-EET (319.0→219.0) are similar, retention times for these two molecules allowed their detection (Supplemental Fig. (**2**)).

Thus, in different experiments using different methods of detection, injection of L-4F reproducibly decreased plasma levels of oxidized fatty acids that are known to bind with high affinity to L-4F compared to apoA-I (15-HETE, 9-HODE, and 13-HODE) [17] while the plasma levels of 20-HETE which binds with equal affinity to L-4F and apoA-I did not change, and the plasma levels of the vasorelaxant and anti-inflammatory 14,15-EET actually increased.

We next examined whether L-4F injection affected renal function, intravascular volume or plasma non-oxidized fatty acids levels. We previously reported that chronic administration of D-4F did not influence renal function [27]. In order to see the effect of 4F on intravascular volume, we measured serum total protein and albumin levels after administration of L-4F or ABCT, and there was no difference of total protein and albumin levels between the two groups (Supplemental Fig. (**3**)) indicating no dilution by the volume of the injections. We also measured the plasma concentration of arachidonic acid, one of the non-oxidized fatty acids, and compared it between both groups. As expected, there was no difference between two groups confirming that intravascular volume did not change (Supplemental Fig. (**4**)).

Next, we determined the binding of HETEs/HODEs to plasma albumin compared to L-4F. In contrast to the case for L-4F, there was no detectable binding of 12-HETE and 9-HODE to albumin but there was binding of a control (retrocyclin-1) to albumin (Supplemental Fig. (**5a to 5c**)). Finally,

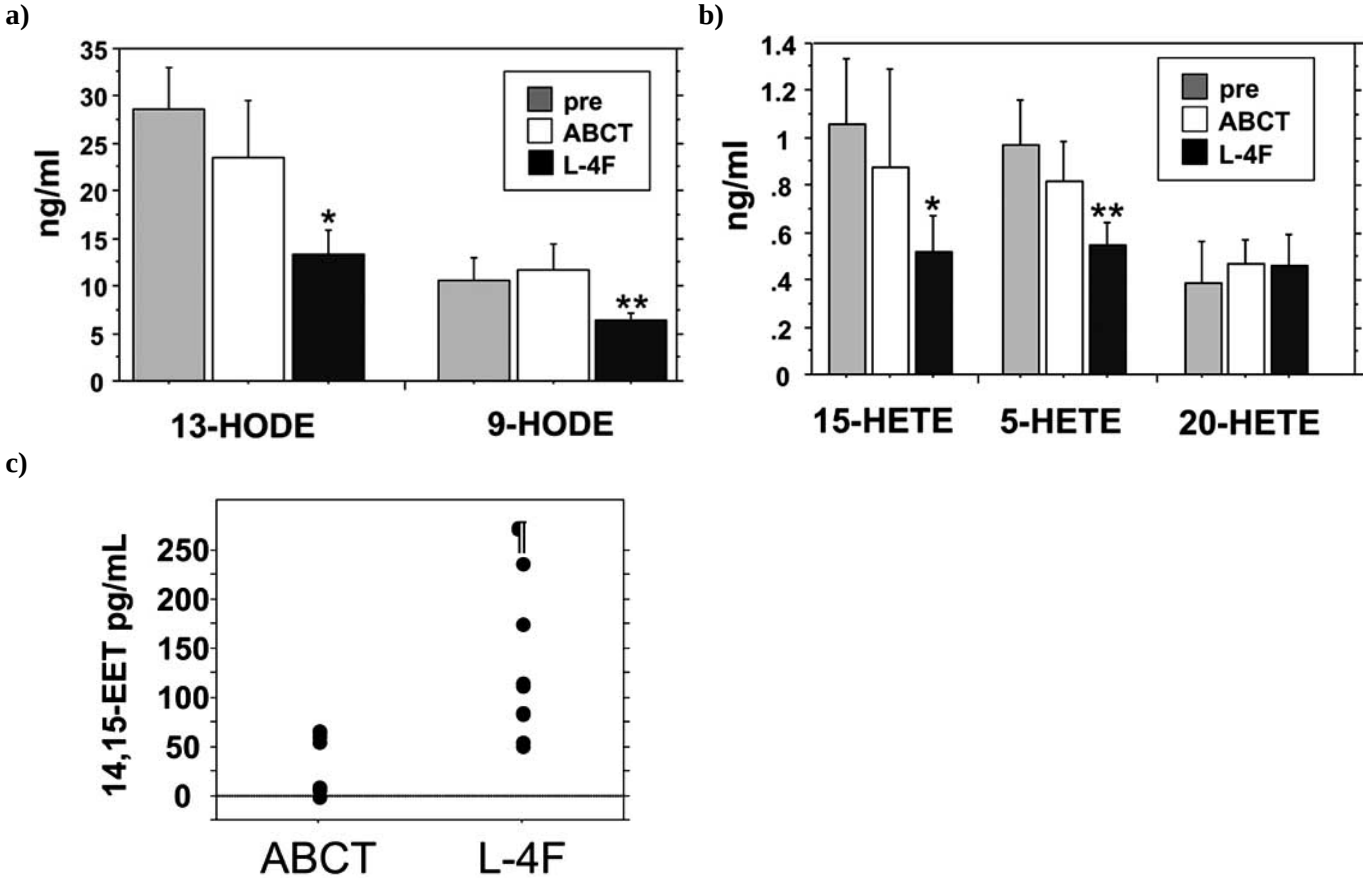

Fig. (3). L-4F treatment differentially reduces plasma HETEs and HODEs levels as measured by LC/MS/MS. ApoE null mice were administered subcutaneously vehicle (ABCT) or vehicle containing L-4F at a dose of 1 mg/kg. After six hours, plasma **a)** 13-HODE and 9-HODE **b)** 15-HETE, 5-HETE, and 20-HETE levels were determined by LC/MS/MS and compared to pre-dose levels. **a)** 13-HODE and 9-HODE. *p<0.0001 vs. pre-dose. **p<0.01 vs. pre-dose. **b)** 15-HETE, 5-HETE and 20-HETE. *p<0.01 vs. pre-dose. **p=0.0003 vs. pre-dose. (a, b; n=6 for each group) **c)** ApoE null mice were injected with vehicle alone (ABCT) or vehicle containing L-4F at a dose of 1 mg/kg. Six hours later the plasma levels of 14,15-EET were determined by LC/MS/MS. (n=8 for each group) ¶p =0.0057 vs. ABCT.

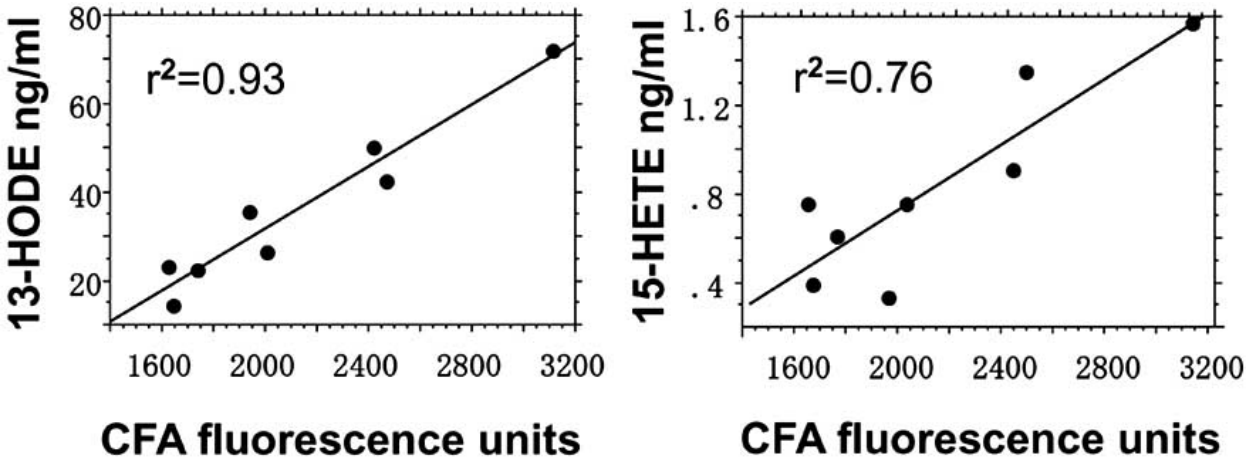

Fig. (4). Correlation of plasma levels of 13-HODE and 15-HETE with a cell-free assay (CFA) for determining HDL-inflammatory properties. ApoE null mice were subcutaneously administered L-4F at a dose of 1 mg/kg. Plasma was obtained pre-dose and 5 or 6 hours after L-4F administration and levels of 13-HODE and 15-HETE were determined by LC/MS/MS and HDL inflammatory properties were determined by the CFA as described in MATERIAL and METHODS. Left panel, r^2=0.93, p<0.0001; right panel, r^2=0.76, p=0.0048.

we measured urine 13-HODE levels to see whether there was increased excretion of oxidized lipids 6 hours after L-4F administration. However, there was no difference in urine 13-HODE levels in mice administered L-4F or buffer alone (ABCT) suggesting that L-4F did not act to increase the excretion of 13-HODE (Supplemental Fig. (**6**)).

Plasma 13-HODE and 15-HETE Levels Correlate with HDL Inflammatory Properties

We previously reported that the fluorescence resulting from the addition of HDL-containing plasma (plasma after removal of apoB-containing proteins) to a standard control LDL is a useful cell-free assay for determining the anti-inflammatory properties of HDL [22]. Therefore, we evaluated the correlation of plasma HDL inflammatory properties measured by this cell-free assay (CFA) with the levels of plasma 13-HODE and 15-HETE after L-4F administration in mice. As shown in the left panel of Fig. (**4**) the levels of plasma 13-HODE strongly correlated with fluorescence levels in the CFA (r^2=0.93, p<0.0001). As shown in the right panel in Fig. (**4**) fluorescence levels in the CFA also correlated with plasma levels of 15-HETE (r^2=0.76).

Plasma 13-HODE and 9-HODE Levels are Increased and HDL Anti-Inflammatory Properties are Decreased after Administration of 13(*S*)-HPODE *In Vivo*, and they are Improved by L-4F Administration

We previously reported [5] that *in vitro* the fatty acid hydroperoxide HPODE has extraordinary potency to oxidize lipids (i.e. HPODE was 200-times more potent than H_2O_2). We also reported [17] that the apolipoprotein mimetic peptide L-4F has very high affinity for 13(*S*)-HPODE (K*D* = 17 ± 4 nM). Therefore, we hypothesized that administration of 13(*S*)-HPODE *in vivo* might increase the levels of plasma oxidized fatty acids and reduce the anti-inflammatory properties of HDL. We also hypothesized that L-4F administration might mitigate the actions of 13(*S*)-HPODE *in vivo*. To test these hypotheses wild-type C57BL/6J mice were injected subcutaneously on the back with 200 μL of vehicle containing 0, 0.75, 1.5, 3, 6 μg 13(*S*)-HPODE per mouse. As shown in Fig. (**5a**) 13(*S*)-HPODE administration dose-dependently reduced the anti-inflammatory properties of the mouse HDL as determined in the cell-based assay. Next, wild-type C57BL/6J or wild-type C3H/HeJ mice were injected subcutaneously on the back with vehicle alone or vehicle containing 3 μg 13(*S*)-HPODE per mouse. Almost simultaneously each mouse received an injection of 200 μL of vehicle with or without L-4F at a dose of 1 mg/kg at a different site from where the 13(*S*)-HPODE was injected. One hour later blood was drawn and plasma levels of 13-HODE or 9-HODE were measured by LC/MS/MS Fig. (**5b** and **5c**). Administration of 13(*S*)-HPODE significantly increased plasma levels of 13-HODE and 9-HODE in atherosclerosis susceptible C57BL/6J mice Fig. (**5b**). Following injection of 13(*S*)-HPODE subcutaneously on the back of the atherosclerosis resistant C3H/HeJ mice, there was a slight but significant increase in plasma levels of 13-HODE Fig. (**5c**). While there was a trend toward increased levels of 9-HODE in the C3H/HeJ mice following injection of 13(S)-HPODE, the increase did not reach significance Fig. (**5c**). Almost simultaneous administration of L-4F at a different site from that where the 13(*S*)-HPODE was administered prevented the increase in plasma levels of 13-HODE and 9-HODE after administration of 13(*S*)-HPODE Fig. (**5b** and **5c**). The same protocol was followed in a separate group of mice except that L-4F was injected intraperitoneally and 6 hours after injection, HDL was isolated from the mice and HDL anti-inflammatory properties were determined in the cell-based assay Fig. (**5d**). Administration of 13(*S*)-HPODE significantly reduced the anti-inflammatory properties of the HDL of both wild-type C57BL/6J and wild-type C3H/HeJ mice. Almost simultaneous administration of L-4F at a different site [a site different from where the 13(*S*)-HPODE was injected] significantly improved HDL anti-inflammatory properties in both strains Fig. (**5d**).

We also studied the effect of 13(S)-HPODE and L-4F administration on total HETEs/HODEs by hydrolyzing the samples as described in the Materials and Methods. Plasma

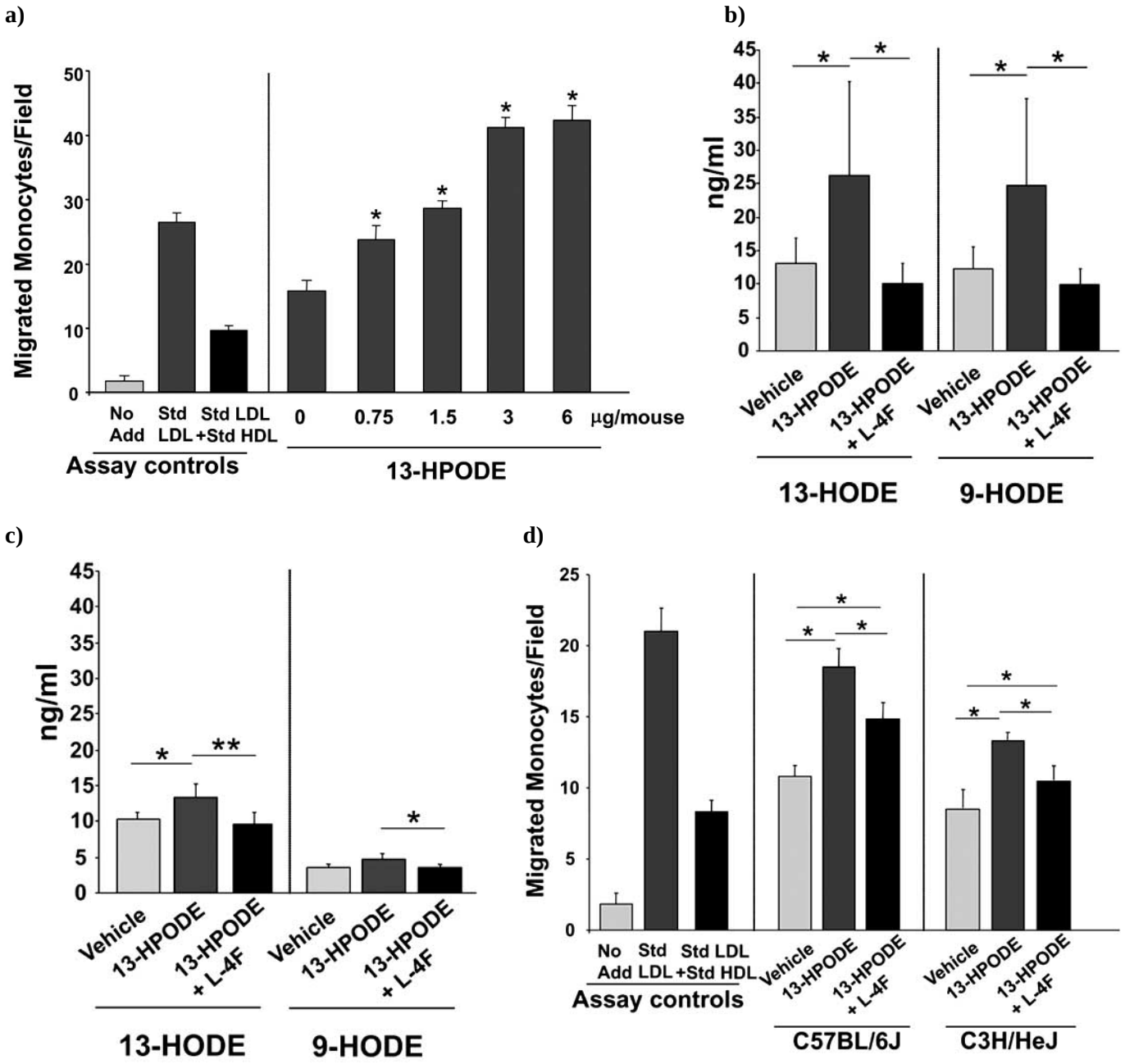

Fig. (5). 13(*S*)-HPODE administration increases plasma 13-HODE and 9-HODE levels, and decreases HDL anti-inflammatory properties all of which are improved by administration of L-4F. **a)** Wild-type C57BL/6J mice were injected subcutaneously on the back with 200 μL of vehicle (ABCT) containing 0, 0.75, 1.5, 3, 6 μg 13(*S*)-HPODE per mouse. Six hours later HDL was isolated from the mice and added to cultures of human aortic endothelial cells that were exposed to a standard control human LDL and monocyte chemotactic activity were determined by a bioassay as described in MATERIALS and METHODS. The left panel of the figure shows the assay controls, i.e. the values for no addition (No Add), the values for addition of the standard control human LDL without HDL (Std LDL) and the values obtained after adding the standard control human LDL to the cells together with a standard control human anti-inflammatory HDL (Std LDL + Std HDL). The values in the right panel of the figure indicate on the X-axis the dose of 13(*S*)-HPODE administered and on the Y-axis the values obtained in the assay after addition of the standard control human LDL together with mouse HDL from each dose group. (n=4 for each dose of 13(*S*)-HPODE) *p<0.05 compared to zero μg 13(*S*)-HPODE; **b)** C57BL/6J mice (n=3-5 for each group) and **c)** C3H/HeJ mice (n=4 for each group) were injected subcutaneously on the back with 200 μL of vehicle (saline) or vehicle containing 3 μg 13(*S*)-HPODE per mouse. Each mouse simultaneously received 200 μL of vehicle (ABCT) with or without L-4F at a dose of 1 mg/kg administered by subcutaneous injection at a different site [a site different from where the 13(*S*)-HPODE was injected]. One hour later plasma levels of 13-HODE and 9-HODE were determined by LC/MS/MS as described in MATERIALS and METHODS. *p<0.05; **p=0.0106. **d)** In a separate group of mice the same protocol was performed as described in panels **b** and **c** except L-4F was injected intraperitoneally and 6 hours after injection HDL was isolated from the mice. HDL inflammatory properties were determined by bioassay as in panel **a** and as described in MATERIALS and METHODS. (n=4 for each group) *p<0.05.

total HETEs/HODEs were 3 to 20 times higher than free HETEs/ HODEs (supplemental Fig. (**7**) for representative total 13-HODE and 15-HETE). In contrast to the results on free HETEs/HODEs there was no effect of injection of L-4F on total HETEs/HODEs (supplemental Fig. (**7**) indicating that the action of L-4F is specific for free HETES/HODEs). To study whether pro-inflammatory changes of HDL require the injection of 13(S)-HPODE (the hydroperoxy form), we tested 13(S)-HODE (the hydroxy form) instead of 13(S)-HPODE. There was no change in the anti-inflammatory properties of the HDL after 13(S)-HODE administration (supplemental Fig. (**8**) indicating that the hydroperoxy form is required).

Next, we studied whether 13(S)-HPODE was present in plasma of the mice after 13(S)-HPODE injection. Although by LC/MS/MS we could easily detect 13(S)-HPODE standard (supplemental Fig. (**9**)), we couldn't detect 13-HPODE after 13(S)-HPODE injection (data not shown), suggesting 13(S)-HPODE is rapidly reduced after injection into the mice.

4F Prevents the HPODE-Mediated Conversion of Normal HDL into Proinflammatory HDL

To determine whether 4F can prevent the HPODE-mediated conversion of normal HDL into proinflammatory HDL, we performed *in vitro* incubation experiments using HDL, 13(*S*)-HPODE and D-4F. D-4F is apoA-I mimetic peptide synthesized from D-amino acids and has been shown to reduce atherosclerosis in mice. Although we couldn't see any change in apoA-I by SDS-PAGE analysis Fig. (**6a**) we found that 0.5 μg/ml of 13(*S*)-HPODE denatured the apoA-I protein in the HDL when analyzed by native-PAGE Fig. (**6b**). This HDL was dysfunctional as shown by its reduced ability to mediate cholesterol efflux Fig. (**6c**). Incubation of HDL with 13(*S*)-HPODE and D-4F (0.5 μg/ml) prevented the denaturation of apoA-I Fig. (**6b** and **6d**) and prevented the loss of the ability of HDL to promote cholesterol efflux Fig. (**6c**). However, adding the D-4F after the incubation of HDL with 13(*S*)-HPODE did not reverse the 13(*S*)-HPODE-mediated changes to apoA-I Fig. (**6d**).

DISCUSSION

Using both ELISA and LC/MS/MS, we have demonstrated that administration of the apoA-I mimetic peptide L-4F significantly reduced plasma 15-HETE, 5-HETE, 13-HODE, and 9-HODE levels, did not change 20-HETE levels, and significantly increased 14,15-EET levels within 6 hours of injection into apoE null mice. The binding affinities of the HETEs/HODEs which were found to be decreased after L-4F administration were much higher for L-4F compared to apoA-I. In contrast, the binding affinity of 20-HETE for L-4F was similar to apoA-I [17]. These data are consistent with the hypothesis that L-4F removes oxidized lipids from plasma that bind with much higher affinity to L-4F compared to apoA-I but will not remove lipids that bind equally well to apoA-I and L-4F. The latter is not unexpected since the maximal plasma concentration of L-4F at the dose administered produces plasma levels of ~ 2.0 μM compared to the concentration of apoA-I in the plasma of apoE null mice of ~35 μM [28].

While we did not measure the binding affinity of EETs for L-4F or apoA-I, it would be difficult to understand how differences in binding affinities to L-4F or apoA-I could result in increased plasma levels following L-4F administration. In any event, the increased plasma levels of EET following L-4F administration are consistent with the known anti-inflammatory properties of L-4F. Sacerdoti *et al*. [29] reported that EETs stimulate heme oxygenase-1 (HO-1) in endothelial cells and Sodhi *et al*. [30] have reported that treatment of heme oxygenase-2 null mice with a dual activity EET-agonist/soluble epoxide hydrolase inhibitor increased renal and vascular EET levels and HO-1 expression. Abraham and colleagues [31-34] have also reported that a number of the anti-inflammatory properties of the 4F peptides are due to the ability of these peptides to increase HO-1. EET levels are largely controlled by soluble epoxide hydrolase which converts EETs to dihydroxyeicosatrienoic acids [15]. Future studies will be needed to determine if L-4F may act directly or indirectly on soluble epoxide hydrolase to increase plasma levels of EETs.

The reduction in plasma oxidized fatty acid levels was not accompanied by an increase in urinary excretion of 13-HODE (Supplemental Fig. (**6**)) suggesting that the removal of the oxidized fatty acids from the plasma was likely associated with metabolism of the oxidized fatty acids in the tissues or excretion in the bile. Future studies will be needed to determine the precise mechanism(s).

In vivo fatty acid hydroperoxides, such as 13(*S*)-HPODE, are immediately reduced to more stable secondary products as HETEs/HODEs. *In vivo* 13-HODE is produced by the reduction of 13(*S*)-HPODE, and it is perhaps not surprising that we observed 13-HODE increase after 13(*S*)-HPODE administration. However, it was unexpected that the plasma 9-HODE level increased to the same extent as 13-HODE in wild-type C57BL/6J mice Fig. (**5b**). The fact that the increase in plasma levels of 13-HODE and 9-HODE were much less in atherosclerosis-resistant C3H/HeJ mice Fig. (**5c**) suggests that their resistance to atherosclerosis may in part be due to resistance to potent lipid oxidants such as 13(*S*)-HPODE. Administration of 13(*S*)-HPODE significantly reduced the anti-inflammatory properties of the HDL of both C57BL/6J and C3H/HeJ mice. However, the change in HDL anti-inflammatory properties following administration of 13(*S*)-HPODE to C3H/HeJ mice was less than in C57BL/6J mice similar to the differences in the plasma levels of 13-HODE and 9-HODE after injection of 13(*S*)-HPODE into these strains. In both strains, administration of L-4F significantly improved HDL anti-inflammatory properties Fig. (**5d**).

In vitro experiments demonstrated that 4F can prevent HPODE-mediated conversion of normal HDL into proinflammatory HDL Fig. (**6**). Taken together with the data showing a strong correlation between HDL anti-inflammatory properties and plasma levels of 13-HODE and 15-HETE Fig. (**4**) the data in this manuscript suggest that L-4F differentially alters plasma levels of oxidized fatty acids resulting in more anti-inflammatory HDL.

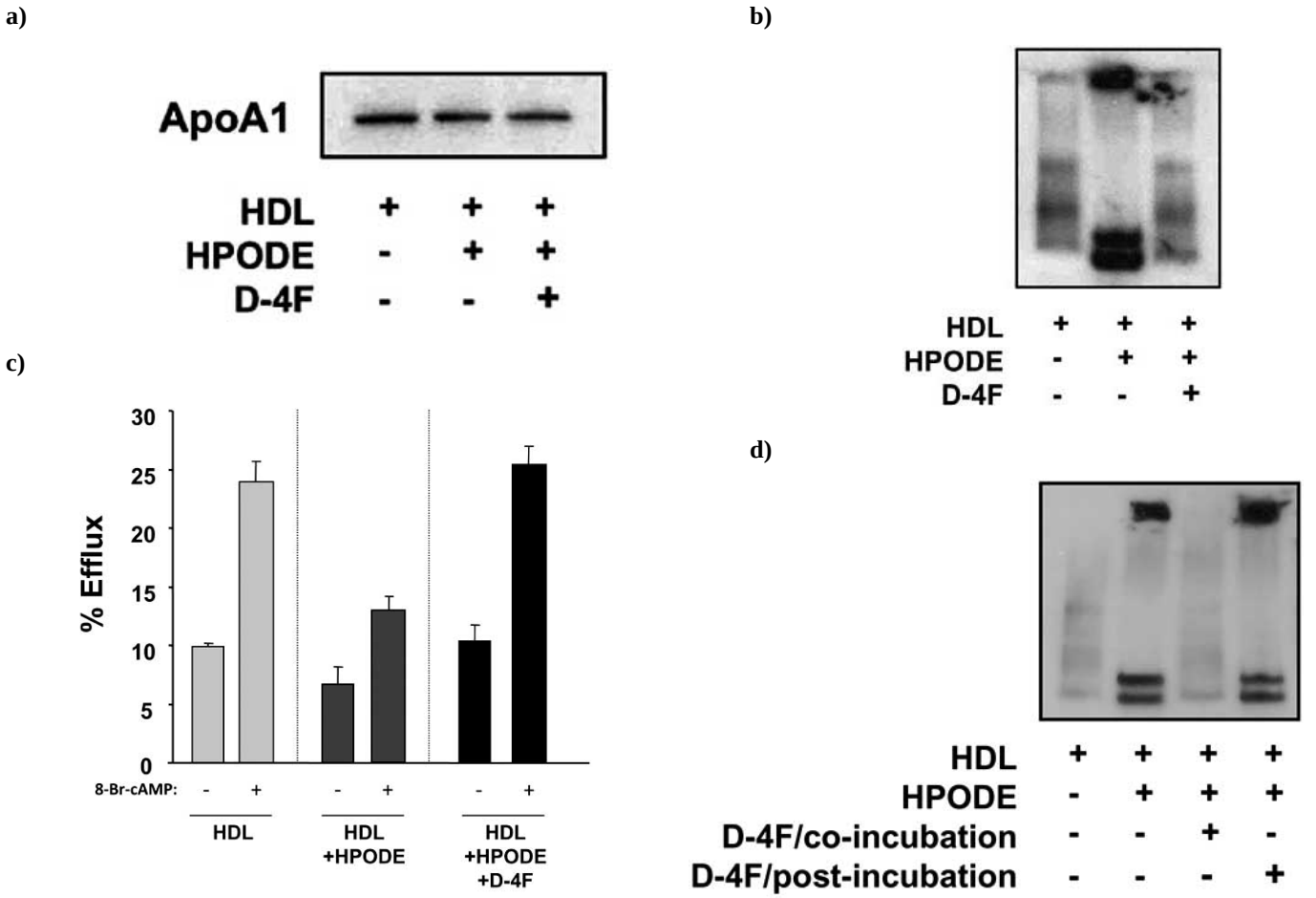

Fig. (6). 4F prevents the HPODE-mediated conversion of normal HDL into proinflammatory HDL. Human HDL (5ug HDL-cholesterol/ml) was incubated alone, or with 0.5 μg/ml of 13(S)-HPODE, or with 0.5 μg/ml of 13(S)-HPODE and 0.5 μg/ml of D-4F for 30 min and subjected to a) SDS-PAGE analysis or b) native-PAGE analysis. The gels were then subjected to Western analysis with anti-human apoA-I antibody. c) After the *in vitro* incubation, HDL was added to RAW264.7 macrophages and cholesterol efflux was determined as described in Materials and Methods in the presence or absence of 8-Bromo-cAMP (0.1mM) pretreatment to maximally stimulate the ABCA1 pathway. d) Human HDL (5 μg HDL-cholesterol/ml) was incubated alone, or with 13(S)-HPODE (0.5 μg/ml), or with 13(S)-HPODE (0.5 μg/ml) and D-4F (0.5 μg/ml) for 60 min (co-incubation), or with 13(S)-HPODE (0.5 μg/ml) for 30 min and then with D-4F (0.5 μg/ml) for 30 min (post-incubation). HDL was subjected to native-PAGE analysis and analyzed by Western with anti-human apoA-I antibody.

ACKNOWLEDGMENTS

Disclosures: MN, STR, GMA and AMF are principals in Bruin Pharma and AMF is an officer in Bruin Pharma.

GRANT SUPPORT

This work was supported in part by US Public Health Service grants HL-30568, HL-34343, HL 082823, and the Laubisch, Castera, and M.K. Grey Funds at UCLA.

SUPPLEMENTARY MATERIAL

Supplementary material is available on the publishers Web site along with the published article.

ABBREVIATIONS

HETEs = Hydroxy-eicosatetraenoic acids

HODEs = Hydroxy-octadecadienoic acids

EETs = Epoxyeicosatrienoic acids

HPETE = Hydroperoxy-eicosatetraenoic acid

HPODE = Hydroperoxy-octadecadienoic acids

LOX = Lipoxygenase

COX = Cyclooxygenase

CYP = Cytochrome P450

REFERENCES

[1] Sigari, F.; Lee, C.; Witztum, J.L. Reaven PD. Fibroblasts that over-express 15-lipoxygenase generate bioactive and minimally modified LDL. *Arterioscler Thromb. Vasc. Biol.*, **1997**, *17*, 3639-3645.

[2] Sakashita, T.; Takahashi, Y.; Kinoshita, T.; Yoshimoto, T. Essential involvement of 12-lipoxygenase in regiospecific and stereospecific oxidation of low density lipoprotein by macrophages. *Eur. J. Biochem.*, **1999**, *265*, 825-831.

[3] Parthasarathy, S.; Litvinov, D.; Selvarajan, K.; Garelnabi, M. Lipid peroxidation and decomposition—conflicting roles in plaque vulnerability and stability. *Biochim. Biophys. Acta.*, **2008**, *1781*, 221-231.

[4] Navab, M.; Hama, S.Y.; Cooke, C.J.; Anantharamaiah, G.M.; Chaddha, M.; Jin, L.; Subbanagounder, G.; Faull, K.F.; Reddy,

S.T.; Miller, N.E.; Fogelman, A.M. Normal high density lipoprotein inhibits three steps in the formation of mildly oxidized low density lipoprotein: step 1. *J. Lipid Res.*, **2000**, *41*, 1481-1494.

[5] Navab, M.; Hama, S.Y.; Anantharamaiah, G.M.; Hassan, K.; Hough, G.P.; Watson, A. D.; Reddy, S.T.; Sevanian, A.; Fonarow, G.C.; Fogelman, A.M. Normal high density lipoprotein inhibits three steps in the formation of mildly oxidized low density lipoprotein: steps 2 and 3. *J. Lipid Res.*, **2000**, *41*, 1495-1508.

[6] Folick, V.A.; Nivar-Aristy, R.A.; Krajewski, L.P.; Cathcart, M.K. Lipoxygenase contributes to the oxidation of lipids in human atherosclerotic plaques. *J. Clin. Invest.*, **1995**, *96*, 504-510.

[7] Funk, C.D.; Cyrus, T. 12/15-lipoxygenase, oxidative modification of LDL and atherogenesis. *Trends Cardiovasc. Med*., **2001**, *11*, 116-124.

[8] Kuhn, H.; Belkner, J.; Zaiss, S.; Fahrenklemper, T.; Wohlfeil, S. Involvement of 15-lipoxygenase in early stages of atherogenesis. *J. Exp. Med*., **1994**, *179*, 1903-1911.

[9] Cyrus, T.; Witztum, J.L.; Rader, D.J.; Tangirala, R.; Fazio, S.; Linton, M.F.; Funk, C.D. Disruption of the 12/15-lipoxygenase gene diminishes atherosclerosis in apo E-deficient mice. *J. Clin. Invest.*, **1999**, *103*, 1597-1604.

[10] George, J.; Afek, A.; Shaish, A.; Levkovitz, H.; Bloom, N.; Cyrus, T.; Zhao, L.; Funk, C.D.; Sigal, E.; Harats, D. 12/15-Lipoxygenase gene disruption attenuates atherogenesis in LDL receptor-deficient mice. *Circulation*, **2001**, *104*, 1646-1650.

[11] Patricia, M.K.; Kim, J.A.; Harper, C.M.; Shih, P.T.; Berliner, J.A.; Natarajan, R.; Nadler, J.L.; Hedrick, C.C. Lipoxygenase products increase monocyte adhesion to human aortic endothelial cells. *Arterioscler. Thromb. Vasc. Biol*., **1999**, *19*, 2615-2622.

[12] Mallat, Z.; Nakamura, T.; Ohan, J.; Leseche, G.; Tedgui, A.; Maclouf, J.; Murphy, R.C. The relationship of hydroxyeicosatetraenoic acids and F2-isoprostanes to plaque instability in human carotid atherosclerosis. *J. Clin. Invest.*, **1999**, *103*, 421-427.

[13] Shishehbor, M.H.; Zhang, R.; Medina, H.; Brennan, M.L.; Brennan, D.M.; Ellis, S.G.; Topol, E.J.; Hazen, S.L. Systemic elevations of free radical oxidation products of arachidonic acid are associated with angiographic evidence of coronary artery disease. *Free Radic.Biol. Med*., **2006**, *41*, 1678-1683.

[14] Sarkis, A. ; Lopez, B. ; Roman, R.J. Role of 20-hydroxyeicosatetraenoic acid and epoxyeicosatrienoic acids in hypertension. *Curr. Opin. Nephrol. Hypertens*, **2004**, *13*, 205-214.

[15] Spector, A. Arachidonic acid cytochrome P450 epoxygenase pathway. *J. Lipid Res*., **2009**, *50*, S52-S56.

[16] Navab, M.; Anantharamaiah, G.M.; Reddy, S.T.; Fogelman, A.M. Apolipoprotein A-I mimetic peptides and their role in atherosclerosis prevention. *Nat. Clin. Pract. Cardiovasc. Med*., **2006**, *3*, 540-547.

[17] Van Lenten, B.J.; Wagner, A.C.; Jung, C.L.; Ruchala, P.; Waring, A.J., Lehrer, R.I.; Watson, A.D.; Hama, S.; Navab, M.; Anantharamaiah, G.M.; Fogelman, A.M. Anti-inflammatory apoA-I-mimetic peptides bind oxidized lipids with much higher affinity than human apoA-I. *J. Lipid Res.*, **2008**, *49*, 2302-2311.

[18] Navab, M.; Anantharamaiah, G.M.; Hama, S.; Garber, D.W.; Chaddha, M.; Hough, G.; Lallone, R.; Fogelman, A.M. Oral administration of an Apo A-I mimetic Peptide synthesized from D-amino acids dramatically reduces atherosclerosis in mice independent of plasma cholesterol. *Circulation*, **2002**, *105*, 290-292.

[19] Peterson, S.J.; Drummond, G.; Kim, D.H.; Li, M.; Kruger, A.L.; Ikehara, S.; Abraham, N.G. L-4F treatment reduces adiposity, increases adiponectin levels, and improves insulin sensitivity in obese mice. *J. Lipid Res.*, **2008**, *49*, 1658-1669.

[20] Folch, J.; Lees, M.; Sloane Stanley, G.H. A simple method for the isolation and purification of total lipides from animal tissues. *J. Biol. Chem.*, **1957**, *226*, 497-509.

[21] Bligh, E.G.; Dyer, W.J. A rapid method of total lipid extraction and purification. *Can. J. Biochem. Physiol.*, **1959**, *37*, 911-917.

[22] Navab, M.; Hama, S.Y.; Hough, G.P.; Subbanagounder, G.; Reddy, S.T.; Fogelman, A.M. A cell-free assay for detecting HDL that is dysfunctional in preventing the formation of or inactivating oxidized phospholipids. *J. Lipid Res.*, **2001**, *42*, 1308-1317.

[23] Van Lenten, B.J.; Wagner, A.C.; Navab, M.; Anantharamaiah, G.M.; Hama, S.; Reddy, S.T.; Fogelman, A.M. Lipoprotein inflammatory properties and serum amyloid A levels but not cholesterol levels predict lesion area in cholesterol-fed rabbits. *J. Lipid Res*., **2007**, *48*, 2344-2353.

[24] Watanabe, J.; Chou, K.J.; Liao, J.C.; Miao, Y,.;Meng, H-H.; Ge, H.; Grijalva, V.; Hama, S.; Kozak, K.; Buga, G.; Whitelegge, J.P.; Lee, T.D.; Faris-Eisner, R.; Navab, M.; Fogelman, A.M.; Reddy, S.T. Differential association of hemoglobin with proinflammatory high density lipoproteins in atherogenic/hyperlipidemic mice. A novel biomarker of atherosclerosis. *J. Biol. Chem.*, **2007**, *282*, 23698-23707.

[25] Cruz, D.; Watson, A.D.; Miller, C.S.; Montoya, D.; Ochoa, M-T.; Sieling, P.A.; Gutierrez, M.A.; Navab, M.; Reddy, S.T. Witztum, J.L.; Fogelman, A.M.; Rea, T.H.; Eisenberg, D.; Berliner, J.; Modlin, R.L. Host-derived oxidized phospholipids and HDL regulate innate immunity in human leprosy. *J. Clin. Invest.*, **2008**, *118*, 2917-2928.

[26] Forte, T.M.; Subbanagounder, G.; Berliner, J.A.; Blanche, P.J.; Clermont, A.O.; Jia, Z.; Oda, M.N.; Krauss R.M.; Bielicki, J.K. Altered activities of anti-atherogenic enzymes LCAT, paraoxonase, and platelet-activating factor acetylhydrolase in atherosclerosis-susceptible mice. *J. Lipid Res.*, **2002**, *43*, 477-485.

[27] Buga, G.M.; Frank, J.S.; Mottino, G.A.; Hakhamian, A.; Narasimha, A.; Watson, A.D.; Yekta, B.; Navab, M.; Reddy, S.T., Anantharamaiah, G.M.; Fogelman, A.M. D-4F reduces EO6 immunoreactivity, SREBP-1c mRNA levels, and renal inflammation in LDL receptor-null mice fed a Western diet. *J. Lipid Res*., **2008**, *49*, 192-205.

[28] Navab, M.; Shechter, I.; Anantharamaiah, G.M.; Reddy, S.T.; Van Lenten, B.J.; Fogelman, A.M. Structure and function of HDL mimetics. *Arterioscler Thromb. Vasc. Biol*., **2010**, *30*, 164-168.

[29] Sacerdoti, D.; Colombrita, C.; Di Pascoli, M.; Schwartzman, M.L.; Bolognesi, M.; Falck, J.R.; Gatta, A.; Abraham, N.G. 11,12-epoxyeicosatrienoic acid stimulates heme oxygenase-1 in endothelial cells. *Prostaglandins Other Lipid Mediat*., **2007**, *82*, 155-161.

[30] Sodhi, K.; Inoue, K.; Gotlinger, K.H.; Canestraro, M.; Vanella, L.; Kim, D.H.; Manthati, V.L.; Koduru, S.R.; Falck, J.R.; Schwartzman, M.L.; Abraham, N.G. Epoxyeicosatrienoic acid agonist rescues the metabolic syndrome phenotype of HO-2 null mice. *J. Pharmacol. Exp. Ther*., **2009**, *331*, 906-916.

[31] Kruger, A.L.; Peterson, S.; Turkseven, S.; Kaminski, P.M.; Zhang, F.F.; Quan, S.; Wolin, M.S.; Abraham, N.G. D-4F induces heme oxygenase-1 and extracellular superoxide dismutase, decreases endothelial cell sloughing, and improves vascular reactivity in rat model of diabetes. *Circulation*, **2005**, *111*, 3126-3134.

[32] Peterson, S.J.; Husney, D.; Kruger, A.L.; Olszanecki, R.; Ricci, F.; Rodella, L.F.; Stacchiotti, A.; Rezzani, R.; McClung, J.A.; Aronow, W.S.; Ikehara, S.; Abraham, N.G. Long-term treatment with the apolipoprotein A1 mimetic peptide increases antioxidants and vascular repair in type I diabetic rats. *J Pharmacol. Exp. Ther.*, **2007**, *322*. 514-520.

[33] Peterson, S.J.; Drummond, G.; Kim, D.H.; Li, M.; Kruger, A.L.; Ikehara, S.; Abraham, N.G. L-4F treatment reduces adiposity, increases adiponectin levels, and improves insulin sensitivity in obese mice. *J. Lipid Res*., **2008**, *49*, 1658-1669.

[34] Peterson, S.J; Kim, D.H.; Li, M.; Positano, V.; Vanella, L.; Rodella, L.F.; Piccolomini, F.; Puri, N.; Gastaldelli.A.; Kusmic, C.; L'Abbate, A.; Abraham, N.G. The L-4F mimetic peptide prevents insulin resistance through increased levels of HO-1, pAMPK, and pAKT in obese mice. *J. Lipid Res*., **2009**, *50*, 1293-1304.

Received: May 12, 2010 **Revised: May 27, 2010** **Accepted: May 27, 2010**